


The effect of recycled concrete powder (RCP) from precast concrete plant on fresh and mechanical properties of cementitious pastes

J.H.A. Rocha  , M.P. Tinoco,  R.D. Toledo Filho

Civil Engineering Program, Universidade Federal do Rio de Janeiro, COPPE/UFRJ, (Rio de Janeiro, Brazil)
: joaquin.rocha@coc.ufrj.br

Received 29 March 2023
Accepted 05 June 2023
Available on line 03 November 2023

ABSTRACT: This study aims to evaluate the effect of RCP from a precast concrete plant on rheological and mechanical properties of cementitious pastes. In the study, Portland cement was replaced by RCP in 10, 20, and 30% (in mass). The hydration kinetics of cement with RCP was studied through isothermal calorimetry. The fresh properties were assessed using mini-slump test and rotational rheometry. The mechanical properties were evaluated through compression tests and the microstructure was studied using Scanning Electron Microscopy. RCP reduces fluidity of the pastes, by increasing both yield stress and plastic viscosity. The addition of RCP accelerates the hydration of cement, while reducing the released heat. RCP also reduces the compressive strength and elastic modulus of the pastes. The use of RCP as partial substitute for cement is viable, due to its size distribution and specific surface area.

KEY WORDS: Recycled concrete powder; Hydration; Rheology; Compressive strength; Sustainability.

Citation/Citar como: Rocha, J.H.A.; Tinoco, M.P.; Toledo Filho, R.D. (2023) The effect of recycled concrete powder (RCP) from precast concrete plant on fresh and mechanical properties of cementitious pastes. *Mater. Construcc.* 73 [352], e325. <https://doi.org/10.3989/mc.2023.351923>.

RESUMEN: *Efecto de los finos de hormigón reciclado (PHR) de una planta de prefabricados de hormigón sobre las propiedades en estado fresco y mecánicas de pastas cementantes.* El objetivo del estudio es evaluar el PHR proveniente de una planta de hormigón premezclado como reemplazo al cemento Portland. La metodología consistió en la elaboración de pastas, sustituyendo el cemento Portland por PHR al 10, 20 y 30% en peso. La cinética de hidratación del cemento con PHR se estudió mediante calorimetría isotérmica. Las propiedades en estado fresco se evaluaron mediante la prueba de mini-slump y la reometría rotacional. Se realizaron ensayos de compresión y la microestructura se estudió mediante Microscopía Electrónica de Barrido. El PHR reduce la fluidez de las pastas, aumentando el límite elástico y la viscosidad plástica. La adición de PHR acelera la hidratación del cemento, al tiempo que reduce el calor liberado. El PHR también reduce la resistencia a la compresión y el módulo elástico de las pastas. El uso de PHR como sustituto parcial del cemento es viable, debido a su distribución de tamaño y área superficial específica.

PALABRAS CLAVE: Polvo de hormigón reciclado; Hidratación; Reología; Resistencia a la compresión; Sostenibilidad.

Copyright: ©2023 CSIC. This is an open-access article distributed under the terms of the Creative Commons Attribution 4.0 International (CC BY 4.0) License.

1. INTRODUCTION

In the last years, mineral additions have been widely used as partial substitutes for Portland cement, in order to reduce CO₂ emissions and energy consumption of construction industry (1–3). Some examples are ground blast furnace slag (GBFS), fly ash (FA) and silica fume (SF). Recently, new sources of additions have been proposed, such as crude and calcined clays, biomass ash, and residues (4, 5). In all cases, the aim is to develop a cement with low clinker content, without compromising durability and mechanical properties of cement-based materials (6).

Additionally, construction industry also faces challenges related to the generation of construction and demolition wastes (CDW), mainly composed by concrete, bricks, steel, and wood (7). It is estimated that CDW represent between 10 and 30% of the total waste present in landfills, causing negative environmental impacts (8). This waste, however, present high potential for reuse and recycling (9, 10). In recent years, some studies have proposed the use of concrete wastes as aggregates and mineral additions to reduce clinker consumption (11–13).

During the production of recycled concrete aggregates, very fine particles (diameter less than 150 µm) are also produced, which are called recycled concrete powder (RCP) (14, 15). RCP is mainly composed by non-hydrated cement, sand, gravel, and cementitious paste (16). Studies show that RCP has potential to be used as supplementary cementitious material (SCM), due to its pozzolanic and physical effects on cement-based materials (17, 18). Meanwhile, depending on its origin, quality, and fineness of RCP, they can also induce negative effects on fresh and mechanical properties and durability of the pastes (12). Several studies used RCP from demolition of existing buildings (19–21); while other authors produced RCP from controlled laboratory samples (18, 22, 23).

The workability of mixes with recycled concrete powder (RCP) decreases as the substitution rate increases, this is due to the irregular microstructure and increased water demand by the particles (24, 25). Horsakulthai (26) found that RCP as a SCM can be reactive, having an activity index of 87.2% for 28 days; however, RCP increased the porosity and water absorption coefficient of self-leveling mortars. Letelier *et al.* (27) recommended a limited use of RCP (<5%) as a cement substitution with particle size less than 75 µm, in order to maintain the mechanical properties of concrete.

The use of RCP can have different effects on the mechanical and durability properties of cement-based materials. Oliveira *et al.* (15) highlighted that up to 25% replacement of cement by RCP does not significantly modify the compressive strength, tensile strength, and elastic modulus in concrete,

thus representing an ecological alternative. On the other hand, Wu *et al.* (9) indicated that the use of RCP as a partial replacement for Portland cement reduces the content of new hydration products and increases the size of pores in cement-based materials. These last characteristics decrease the compressive strength and promote water transport properties, such as absorption and sorption coefficients, compromising durability.

In general, if the percentages of cement replacement by RCP are low and the particle size is smaller, the mechanical resistance and durability of cement-based materials can be maintained or improved (28–30). However, due to the heterogeneity of the material, more research is needed comparing different origins and sources of the RCP. On the other hand, the environmental benefit of the use of RCP to reduce both the emission of carbon dioxide (CO₂) and the consumption of energy has been verified in the literature (31–33). He *et al.* (32) indicated that up to a 20% RCP could reduce up to 17.5% of CO₂ emissions. Wu *et al.* (34) reported that even RCP with mechanical and thermal treatment (up to 700 °C) can reduce energy and CO₂ emissions.

Although studies on the influence of particle size and substitution percentage have been reported, there are few studies on the use of very fine recycled concrete powders (size distribution close to cement). Furthermore, the source of the RCP has not been widely discussed. Two sources of RCP are reported in the literature, demolition waste from concrete structures (19–21) and laboratory concrete specimens (18, 22, 23), both RCP allow evaluating the impact of heterogeneity on cement-based materials. However, there are no studies on the use of RCP from concrete production plants, which also generate waste during their activities.

In this sense, the present article evaluates the use of RCP from a precast concrete plant as a substitute for Portland cement in cementitious pastes. For this purpose, the following procedure was considered: characterization of the RCP; analysis of the fresh state using mini-slump and rotational rheometry; study of hydration by using isothermal calorimetry; analysis of compressive strength and elastic modulus for 1, 7, 28, and 120 days, and evaluation of the microstructure of the pastes at 1 and 28 days.

2. MATERIALS AND METHODS

2.1. Materials

For the present work, a high-early strength cement, Brazilian type CII-F32 (ASTM cement type II), from LafargeHolcim, was used. According to the manufacturer, the CP II F-32 has 80–90% clinker, 3–5% gypsum and 10–15% fillers, fulfilling the

requirements of the NBR 16697 (35). The RCP consisted of hardened concrete waste collected from a precast concrete plant (RCP-C). The RCP-C initially underwent a sieving process using the material passing through the #100 sieve (150 μm), followed by a grinding process using a ball mill for approximately 30 minutes to obtain a particle size distribution similar to Portland cement, as recommended in literature (12, 36, 37). The ball mill consists of a metal jar (20.5 cm internal diameter and 35 cm internal length), operating at a frequency of 300 rpm (89.7% of the critical speed). Portland cement and RCP-C were chemically and physically characterized. The chemical composition was determined using X-ray fluorescence (XRF) with a Shimadzu EDX-720 spectrometer. Loss on ignition was obtained by heating the materials to 1000°C at a rate of 10°C/min, following the recommendations of NBR NM 18 (38). Density was obtained using helium pycnometer. Particle size distribution was found through laser diffraction. Finally, specific surface area (SSA) was determined using ASTM C204 (39).

2.2. Mix compositions and preparation

Cement pastes were prepared with a w/c ratio of 0.4. Portland cement was replaced by RCP-C in four different percentages: 0 (reference), 10, 20, and 30% (by weight). The replacement values were selected based on recommendations found in literature (12, 24, 26). Table 1 shows the mix proportions used.

TABLE 1. Proportion of materials, by weight, used in this study.

Mixture	Portland cement (%)	RCP-C (%)	a/c
CP	100	0	0.4
C10	90	10	0.4
C20	80	20	0.4
C30	70	30	0.4

The mixing method consisted of three stages: 1) mixing the materials at a speed of 1000 \pm 50 rpm for 2.5 minutes; 2) stop for a minute; and 3) mixing at high speed, 3000 \pm 50 rpm for 2.5 minutes. A Chandler Engineering™ paddle mixer was used for this procedure. The dimensions of the cement pastes were height of 5 cm and diameter of 2.5 cm.

For the cure procedure, the NBR 7215 (40) was followed. The specimens were placed in a humid chamber, where they remained for up to 24 hours (initial cure period). Subsequently, they were removed from the mold and placed immersed in a water tank saturated with lime, where the specimens remained until the age of the test, except for the 1-day specimens. The specimens were smoothed at the ends in order to obtain a flat surface for the compressive strength and modulus of elasticity tests. It was also visually verified that the test bodies did not present cracks on their surface.

2.3. Fresh state properties

Fresh state properties were assessed using mini-slump tests and rotational rheometry. The mini-slump test uses a small truncated-conical mold measuring 60 mm in height and having an upper internal diameter of 20 mm and a lower internal diameter of 40 mm. For the rheological tests, a viscosimeter model HD DV-III Ultra, from Brookfield, equipped with a Vane sprindler (V73), was used. The materials were placed in a 5.63 cm diameter beaker and immediately tested once the mixture was prepared. To determine the flow curves, the shear rate protocol proposed by Tinoco et al. (41) was applied (Figure 1). Under this protocol, the samples went through an initial pre-shear phase of 200s, starting from a shear rate of 0 to 0.2 s⁻¹. Subsequently, in order to ensure the homogeneity of the sample, the shear rate was kept constant at 0.2 s⁻¹ for 70s. Then, the flow curves were obtained by increasing the shear rate up to 42.5 s⁻¹ in 20 stages of 10 s (ascending ramp). Finally, the shear rate was reduced to 0.2 s⁻¹ in 20 stages of 10 s (descending ramp).

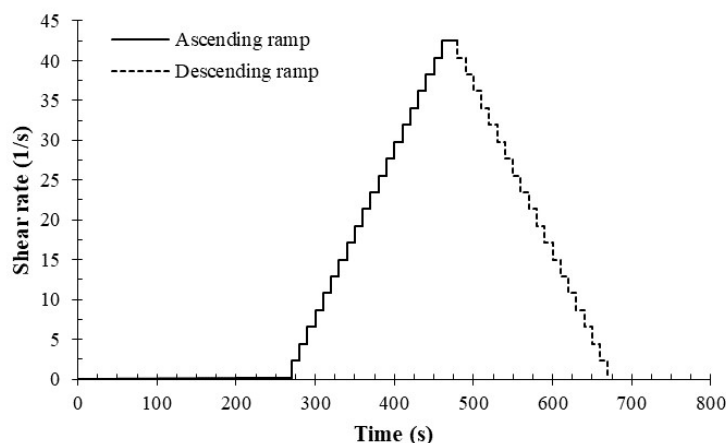


FIGURE 1. Shear rate protocol used for rheological testing. Based on Tinoco et al. (41).

By regression and using the data from the descending flow curve, the dynamic yield stress (τ_0) and plastic viscosity (μ) were obtained. The rheological models of Bingham (Equation [1]) and modified Bingham (Equation [2]) were considered to describe the linear and nonlinear behavior, respectively.

$$\tau = \tau_0 + \mu\dot{\gamma} \quad [1]$$

$$\tau = \tau_0 + \mu\dot{\gamma} + c\dot{\gamma}^2 \quad [2]$$

Where τ is the shear stress (Pa), τ_0 is the dynamic yield stress (Pa), μ is the plastic viscosity (Pa.s), $\dot{\gamma}$ is the shear rate (s^{-1}), and c is a second-order parameter ($Pa.s^2$).

2.4. Isothermal calorimetry

In order to study the effect of RCP-C on the hydration heat, isothermal calorimetry tests were performed. A TAM Air equipment with 8 independent channels (TA Instruments) was used at a temperature of 25°C for 7 days. Deionized water was used as reference material. For the tests, 5g of material was used. For the analysis of results, the initial period (pre-induction) was not considered since the pastes were prepared outside the calorimeter.

2.5. Compression tests

Compressive strength was determined for ages of 1, 7, 28, and 120 days, using 4 specimens per mixture. For the tests, a Shimadzu UH-F (100 kN capacity) mechanical actuator was used, following the recommendations of NBR 7215 (40) were used. The test displacement rate was 0.1 mm/min, maintained constant until the specimen's rupture. Additionally, electric transducers (LVDT) were used to measure longitudinal displacement, which was used to obtain the elastic modulus according to ASTM C469 (42).

2.6. Scanning electron microscopy (SEM)

In order to assess the morphology of the recycled concrete powder (RCP-C) and to visualize the hydration products formed in the 1-day and 28-days pastes, a scanning electron microscope (SEM), model TM3000, from Hitachi, was used.

3. RESULTS AND DISCUSSION

3.1. Materials properties

The chemical composition of Portland cement and RCP-C is presented in Table 2. Both materials have the

same oxides, but the content varies considerably in each material. RCP-C has a higher content of CaO, followed by SiO₂ and Al₂O₃, which may be due to the old hydration products, unhydrated cement particles, and calcite (43). On the other hand, the RCP-C does not meet the requirements of ASTM C618 (44) to be considered a pozzolanic. Although the sum of SiO₂+Al₂O₃+Fe₂O₃ is greater than 50%, it does not meet the criteria of CaO content (18% maximum) and loss on ignition (6% maximum) to be classified as Class F or C pozzolan, respectively. There is no consensus in literature regarding the proportion of chemical composition with respect to recycled concrete powder, which depends on its origin. However, some studies show that demolition RCP has a higher SiO₂ content (15, 26, 45), while laboratory RCP has a higher CaO content (46–48), with RCP-C being closer to the latter source.

TABLE 2. Chemical composition of Portland and RCP-C (in %).

Oxides	CP II F 32	RCP-C
CaO	67.94	36.76
SiO ₂	10.31	34.32
Fe ₂ O ₃	3.98	5.22
Al ₂ O ₃	2.94	8.94
SO ₃	2.94	2.70
K ₂ O	0.37	1.76
SrO	0.32	0.16
TiO ₂	0.30	1.10
MnO	0.08	0.34
ZnO	0.04	0.02
ZrO ₂	0.00	0.19
Rb ₂ O	0.00	0.03
Loss on ignition	10.78	8.47

Figure 2 shows the particle size distribution of Portland cement and RCP-C, indicating a similar granulometry (D_{50}), which suggests that it is suitable for use as SCM (49, 50). Table 3 presents the physical properties of the materials studied. It is observed that RCP-C has finer particles than Portland cement with respect to D_{10} , but also a considerable amount of large particles (D_{90}). It is noteworthy that the specific surface area (SSA) of RCP-C is 2.45 times greater than that of Portland cement. Generally, SSA of RCP reported in the literature is greater than that of Portland cement due to the irregular surface of RCP particles, the presence of hydration products, and calcite (12).

3.2. Fresh state properties

The results of the mini-slump test are presented in Figure 3. Since no superplasticizer was used, the

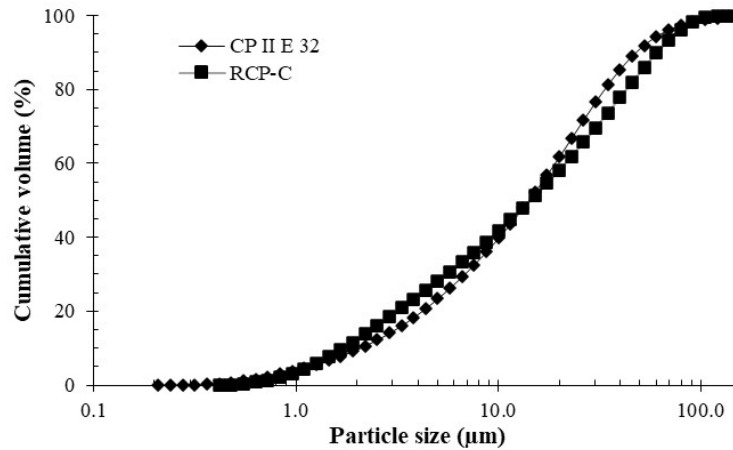


FIGURE 2. Size distributions of Portland cement and RCP-C.

TABLE 3. Physical properties of Portland cement and RCP-C.

Parameter	Cement Portland	RCP-C
D10 (µm)	2.06	1.72
D50 (µm)	14.14	14.42
D90 (µm)	47.79	60.67
Specific gravity (g/cm ³)	3.05	2.68
Specific surface area (cm ² /g)	3762.77	9252.22

fresh state behavior is solely due to the replacement of Portland cement by RCP-C. As the amount of RCP-C increased, the flowability of the pastes considerably decreased, with the spread area decreasing from 41.16 (reference) to 21.15 cm² (C30), a maximum reduction of 48.62%. This behavior is attributed to the fine particles (Figure 4a) and the increase in SSA (requiring more water), the latter caused by the rough surface of RCP-C (Figure 4b) (51–53). Although there is a 48.52% reduction in the spread in the C30 paste compared to the ref-

erence, all the paste were fluid enough not to require mechanical or manual compaction. The ratio of the spreading diameter presented increases with respect to the base of the truncated-conical mold, 80.97, 60.07, 45.25 and 29.72% for CP, C10, C20 and C30, respectively.

Figure 5 shows shear stress vs shear rate results for the pastes with RCP-C. Table 4 summarizes the main fitting parameters of the linear Bingham model and the modified Bingham model (second-degree polynomial). Both for the linear and polynomial models, re-

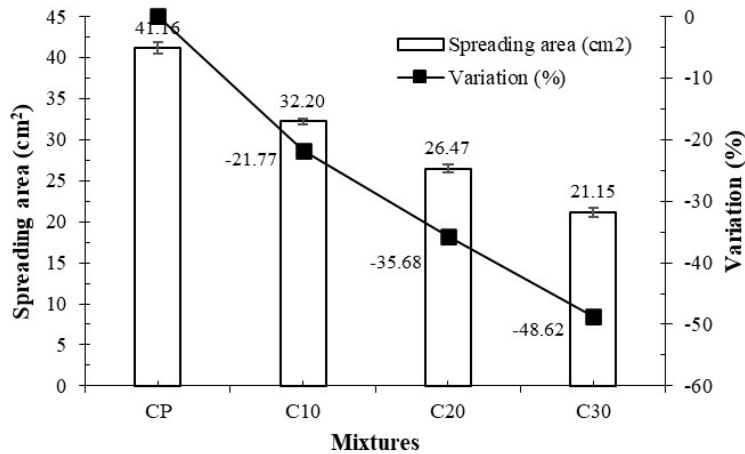


FIGURE 3. Spreading area for the mixtures studied.

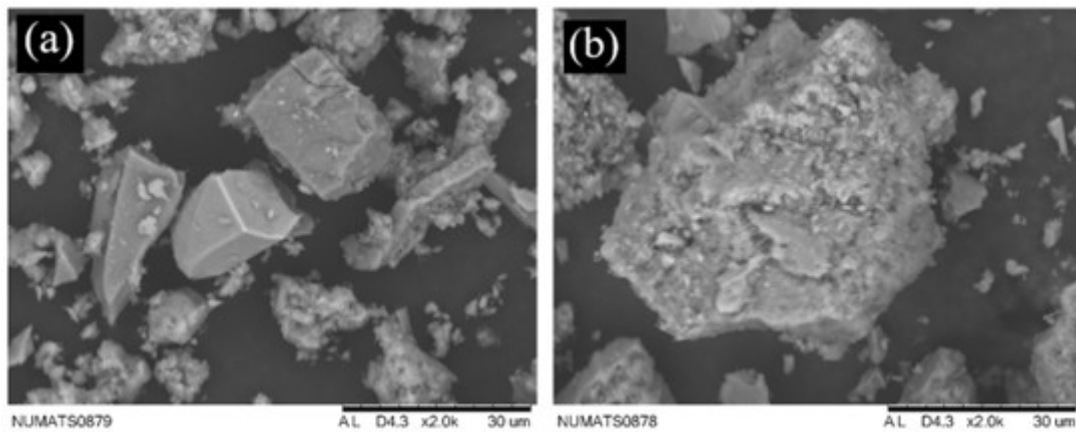


FIGURE 4. Micrographs of RCP-C: (a) Fine particles, and (b) irregular surface of RCP-C.

placing Portland cement with RCP-C increased τ_0 and μ . It is important to highlight that the second-degree polynomial model achieved a better fit of the shear stress curves, $R^2 > 0.99$ in all cases, and was selected for the analysis. On the other hand, the R^2 of the linear model was close to 0.90 for the RCP-C mixes, presenting a lower fit to the flow curves.

Similar to the results of the mini slump tests, it is observed that the use of RCP-C reduced the flowability of the paste, which is attributed to the fine-

ness, irregular morphology, and SSA of the RCP-C (51–53). In this sense, the irregular shape and the increased water demand (higher SSA) made the flow of particles difficult (higher friction), increasing τ_0 and μ , results also reported by Ge *et al.* (54) and Hou *et al.* (21). The τ_0 increased significantly in values of 88.45, 97.48, and 140.34% for 10, 20, and 30% of RCP-C, respectively. In the same sense, μ increased by 65.38, 141.87, and 171.69% for 10, 20, and 30%, respectively.

TABLE 4. Rheological parameters for the Bingham and modified Bingham models.

Mixture	Bingham model			Modified-Bingham model				
	τ_0 (Pa)	μ (Pa.s)	R^2	τ_0 (Pa)	μ (Pa.s)	c (Pa.s ²)	c / μ	R^2
CP	37.433	0.534	0.974	34.795	0.855	-0.007	-0.008	0.995
C10	71.507	0.692	0.938	65.573	1.414	-0.015	0.011	0.998
C20	78.187	0.915	0.913	68.712	2.068	-0.025	-0.012	0.999
C30	94.107	1.007	0.906	83.626	2.323	-0.029	-0.012	0.997

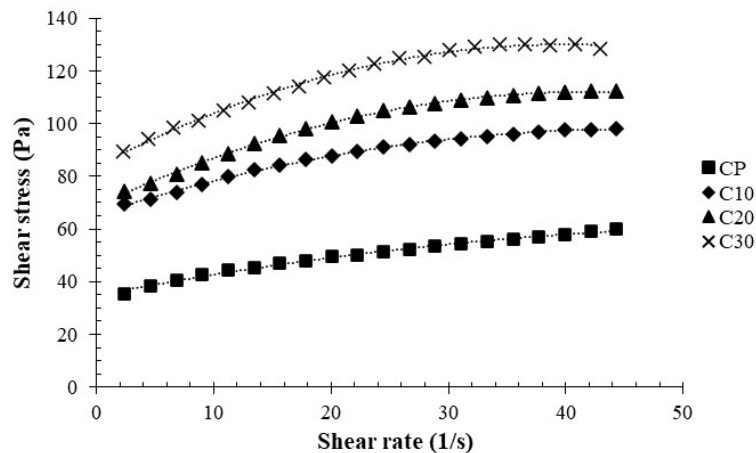


FIGURE 5. Flow curves obtained for the composites studied.

3.3. Isothermal calorimetry

Figures 6a and 6b present the results of heat flow and cumulative heat release for Portland cement and RCP-C blends, respectively. The heat flow curves show that all blends have the same behavior profile, with stages of induction, acceleration, and deceleration. However, it is observed that replacing Portland cement with RCP-C up to 30% reduces the induction period and accelerates the hydration of the pastes in the first few hours (28).

The kinetics during the induction period follow the order C30>C20>C10>CP, but during the acceleration period, the kinetics change between the mixes with RCP-C. These results indicate that RCP-C accelerates the hydration of Portland cement in the first hours, which is attributed to the fine particles (D_{10}) and nucleation effect of RCP-C, with a higher SSA (Table 3) (9, 19, 24, 29, 55). However, the higher heat flow decreases as Portland cement is replaced by RCP-C, CP>C10>C20>C30. The peak of the acceleration phase corresponds to the hydration of C_3S (28), indicating that the dilution effect (lower clinker content) surpasses the nucleation effect of RCP-C (induction stage), even though RCP-C has a higher SSA than Portland cement.

Although the fineness of RCP-C is similar to Portland cement, it only accelerates and increases the heat flow during the first hours for the percentages used. He et al. (31) pointed out that using RCP with a D_{50} of 142 and 4.1 μm reduces the peak heat flow, but when using RCP with a D_{50} of 2.1 μm , the heat flow was higher than the reference. In the same vein, Wang et al. (56) also reported that the intensity of the heat peak improves with fine RCP particles ($D_{50}=0.324 \mu\text{m}$). Therefore, smaller RCP particles ($D_{50}\leq 14.42 \mu\text{m}$) could accelerate and increase the heat flow for a longer period of time. On the other hand, in the deceleration phase, the consumption of sulfate and secondary formation of ettringite (sec-

ond peak) are perceived, which is less pronounced with the addition of RCP-C, also attributed to the reduction of Portland cement (dilution effect) (28, 29).

During the first hours, the accumulated released heat from mixes with RCP-C is slightly higher than the reference. After 3 hours, the accumulated heat is higher by 23.79%, 42.97%, and 6.51% for 10%, 20%, and 30% replacement of Portland cement by RCP-C, respectively. It is observed that the use of RCP-C promotes the hydration of Portland cement by nucleation effect, mainly (21, 32). However, the use of 30% RCP-C resulted in released heat almost equal to the reference, which may be attributed to the high content of coarse particles (D_{90}) that compensated for the nucleation effect. After 72 hours, there is a reduction in the released heat by 6.93%, 14.04%, and 22.71% for 10%, 20%, and 30% RCP-C, respectively. Finally, at the end of the test (7 days), the accumulated released heat of CP, C10, C20, and C30 were 265.96, 245.95 (-7.52%), 227.98 (-14.28%), and 208.42 (-21.63%), respectively. This behavior indicates that the acceleration of hydration in the early hours is not sufficient to compensate for the reduction of Clinker in the mixtures (dilution effect) (11, 32), which could mean a reduction in mechanical properties (56).

In this study, 10% RCP-C presents similar released heat to CP, lower percentages, and greater fineness would promote the hydration reaction (24, 57). Although Liu et al. (58) indicate that replacements up to 30% of Portland cement by RCP decrease the heat flow and accumulated heat, He et al. (32) with a replacement of 30% RCP ($D_{50}=2.1 \mu\text{m}$) reported an increase in the intensity of the heat peak and released heat. Deng et al. (19) indicate that the use of 8% RCP not only reduces the induction period but also promotes released heat. Zhang et al. (28) indicate that the accumulated heat increases in the first hours (12 hours) due to the continuous promotion of cement hydration for 4% RCP with $D_{50}=0.249 \mu\text{m}$.

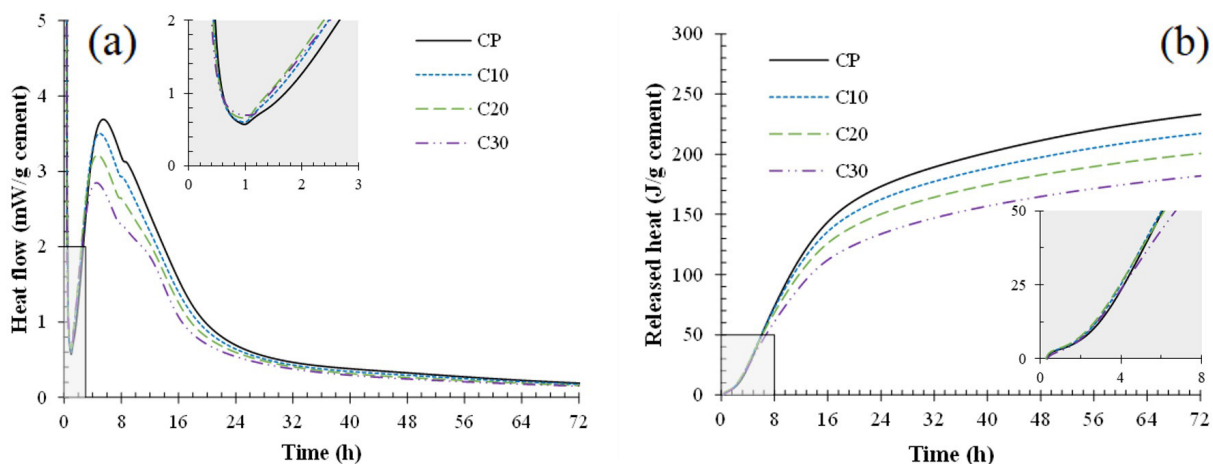


FIGURE 6. Isothermal calorimetry: (a) Heat flow curves, and (b) cumulated heat.

3.4. Compressive strength

Figures 7a and 7b show the results of compressive strength and its variation relative to the reference. For one-day-old mixes, it is observed that the mixes with RCP-C have a notable decrease in compressive strength: 24.48, 33.85, and 42.96 for 10, 20, and 30% replacement of Portland cement with RCP-C, indicating that higher RCP-C content leads to lower compressive strength. While the decreasing trend persists for all ages tested, it can be observed that it is less pronounced for later ages. For 28 days, the reduction is 3.70, 10.85, and 25.56% for 10, 20, and 30%, respectively. These results agree with Wang *et al.* (57), who reported a reduction of 22.3% at 28 days for 30% RCP. For 120 days, the reduction is 31.30, 11.36, and 4.07% for 30, 20, and 10% of RCP-C, similar percentage decreases to 28 days.

The reduction of compressive strength can be attributed to the dilution effect. The lower amount of clinker translates into a decrease in hydration products, resulting in a less compact microstructure (9, 23, 31, 53). This reduction can be also explained by the inert particles in RCP-C (45, 52, 59). As confirmed by isothermal calorimetry (Figure 6), increasing the replacement of Portland cement with RCP-C decreases the heat released by the pastes, which is related to a decrease in the mechanical strength of cement-based materials (51). However, the reduction is only significant at early ages, indicating that the dilution effect prevails during this period (31). For 28 and 120 days, there is minimal reduction for 10 and 20% RCP-C, indicating a possible pozzolanic reaction of RCP-C and, to a lesser extent, rehydration of the old cement particles in RCP-C (26, 45, 60).

Some studies indicate that the content of amorphous SiO_2 and Al_2O_3 particles can react with CH to form CSH and CASH gel, compensating the dilution effect (20, 32). On the other hand, RCP-C microparticles, essentially calcite and quartz, can act as microfillers, increasing the compactness of the pastes (26). In this research, it is observed that this

synergistic effect, pozzolanic reaction, and filler, is positive to compensate for the dilution effect up to 20% RCP-C, a percentage also reported by Chen *et al.* (20). Further addition of RCP-C results in an excessive amount of particles, both unreactive and of lower fineness, which do not compensate for the negative effect of dilution on compressive strength (11, 61).

Tang *et al.* (62) showed that RCP has a limited effect on compressive strength at 28 days due to the pozzolanic reaction and filler effect. While the results presented show this trend, it is important to consider the percentage of substitution and fineness of RCP-C. Xiao *et al.* (24) demonstrated that when the replacement is less than 30%, the effect of RCP is not significant on compressive strength. On the other hand, Liu *et al.* (58) found that using 30% RCP reduced compressive strength. Therefore, this study considered a maximum substitution of 30% to verify its effect on compressive strength. Regarding fineness, He *et al.* (32) found that the negative effect of RCP on compressive strength still had an effect up to $D_{50}=4.1 \mu\text{m}$, but finer particles ($D_{50}=0.324 \mu\text{m}$) refined the cementitious matrix and increased compressive strength. In this regard, Yang *et al.* (29) recommend the use of ultrafine RCP particles to improve compressive strength.

It was observed that 10% and 20% of RCP-C do not significantly influence compressive strength for ages ≥ 28 days. However, replacing 30% of Portland cement with RCP-C resulted in a greater reduction in compressive strength for all tested ages. This indicates that, for the particle size used ($D_{50} = 14.42 \mu\text{m}$), the recommended substitution is 20%. However, using percentages below 10% could maintain or slightly improve compressive strength, a result that agrees with (62). It is recommended to use RCP-C with lower fineness to have a greater physical effect, mainly by maintaining the percentages used (10%, 20%, and 30%).

It is observed that, in the referenced literature, Type I cement was used, which has a higher clinker content, approximately 95-100%. In the pres-

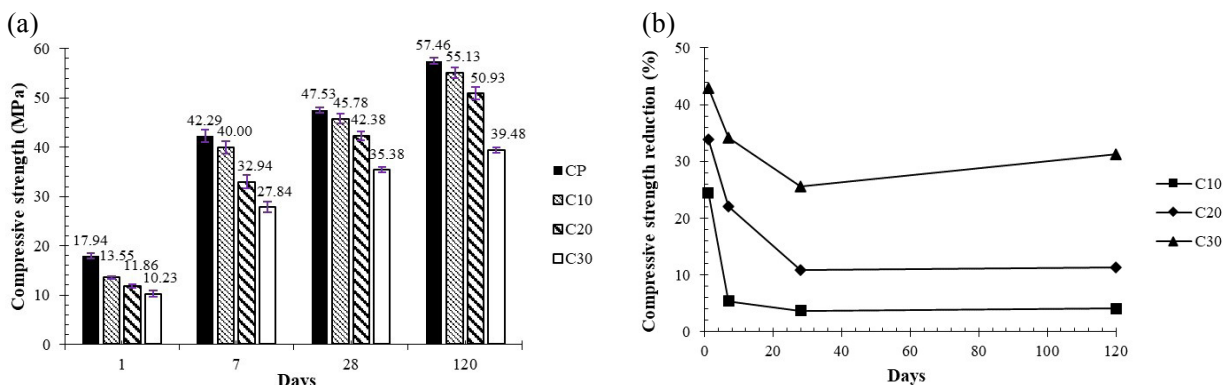


FIGURE 7. Compressive behavior of the pastes: (a) Compressive strength, and (b) Its variation relative to the reference.

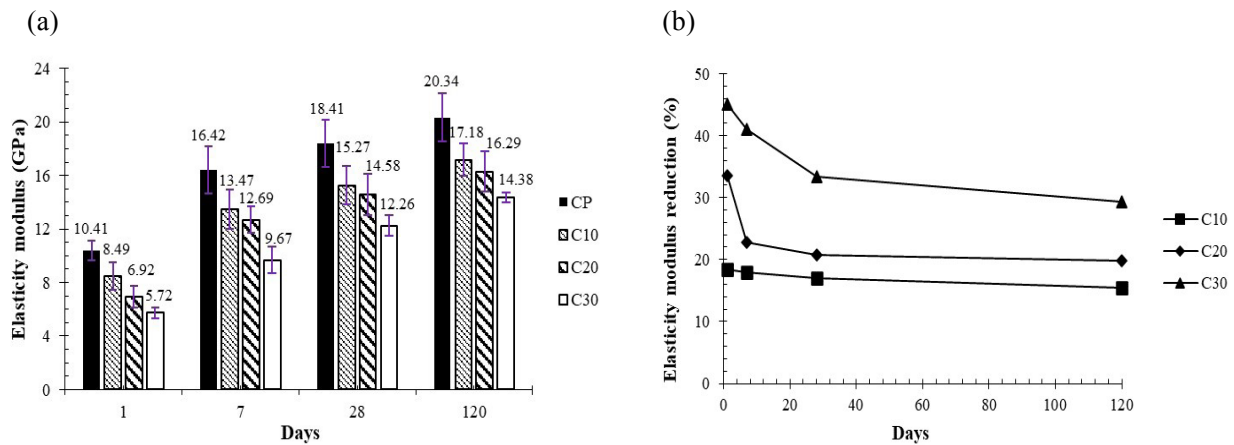


FIGURE 8. (a) Elastic modulus, and (b) Its variation relative to the reference.

ent study, a Type II cement was used with RCP-C, where the content of additions can reach up to 50%. Regardless of the filling and nucleation effect of the RCP-C, the limestone filler of the cement and the RCP-C generate a considerable dilution effect, decreasing the hydration products with a significant impact on the mechanical resistance of the pastes (12, 27, 63, 64), as was verified for the 30% RCP-C paste. For future studies that consider type II cements (with limestone filler) and RCP, a more in-depth analysis of the synergistic effect of both materials is necessary.

3.5. Elastic modulus

The elastic modulus shows the same decreasing trend as compressive strength (Figure 8); the greater the substitution of Portland cement with RCP-C, the lower the elastic modulus developed. For one day, the greatest reduction compared to the reference is observed: 45.01%, 33.56%, and 18.43% for 30%, 20%, and 10% of RCP-C, respectively. For later ages, the percentage of reduction is lower; for example, at 28 days, the decrease is 33.41%, 20.77%, and 17.01% for 30%, 20%, and 10% of RCP-C, respectively. Similar percentages are presented for 120 days.

It is worth noting that 30% of RCP-C has a greater impact on the reduction of the modulus of elasticity at all ages, while 10% and 20% of RCP-C present a lower and similar reduction. This behavior is attributed to the dilution effect of the Clinker, mainly (18, 45, 65). He et al. (31) attribute the reduction of the modulus of elasticity to the low density of RCP particles compared to Portland cement (Table 3). Other authors also indicate that the decrease in the modulus of elasticity is due to RCP particles being less hard and rigid than those of Portland cement (15, 38, 66).

3.6. Microstructure

In Figure 9 the SEM images for the Portland cement mixtures are presented. The same hydration products were identified in all the samples tested. Deng et al. (19) point out that the use of RCP promotes the formation of hydration products, Calcium Hydroxide (CH), Calcium Silicate Hydrates (C-S-H) and ettringite (AFt) from the earliest ages. However, the proportions are different, for example, for the 1-day-old samples, a greater presence of ettringite (AFt) can be distinguished, attributing the initial mechanical resistance (59).

It is important to highlight the presence of AFt in the RCP-C pasts at 28 days. These results agree with other authors, who indicate the stability of the AFt at 28 days (51, 59, 67), even Caneda-Martínez et al. (68) reported AFt in up to 90 days in RCP pastes. The AFt comes from both the hydration reaction of the cement and the RCP-C, previous studies have confirmed the presence of AFt in the composition of the RCP (49, 69). However, in order to determine the amount and origin of the AFt, it is necessary to perform complementary tests, like thermal gravimetric analysis (TGA) and X-ray diffraction (XRD).

In the C10, C20 and C30 mixtures, the presence of C-S-H gel adhered to the surface of the RCP-C particles is observed, indicating the nucleation effect of this powder. However, as described in subtitle 3.3 (Isothermal calorimetry), this effect is only predominant in the first hours of cement hydration. On the other hand, the RCP-C particles observed are large (greater than the D50 of the cement) and crystalline, presenting the effect of clinker dilution, less quantity of hydration products compared to the reference (52). This situation generates a decrease in the development of mechanical resistance, the greater the amount of RCP, the greater the content of large and non-reactive particles.

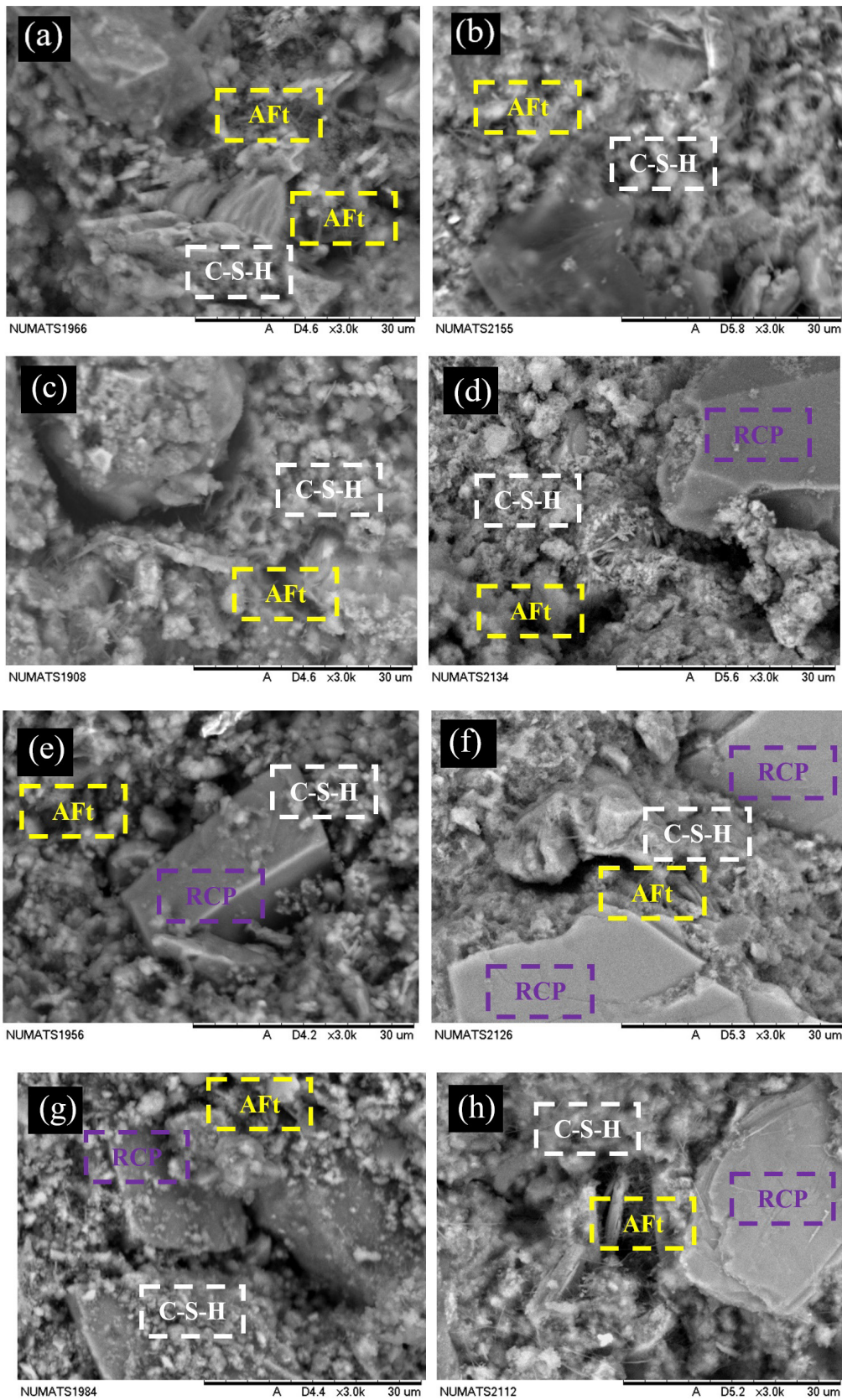


FIGURE 9. Microstructure: (a) 1-day Portland cement paste, (b) 28-days Portland cement paste, (c) 1-day C10 paste, (d) 28-days C10 paste, (e) 1-day C20 paste, (f) 28-days C20 paste, (g) 1-day C30 paste, and (h) 28-days C30 paste.

4. CONCLUSIONS

In the present study, an experimental on the use of RCP-C as mineral addition for cementitious materials was carried out. The RCP-C originated from construction (precast concrete plant), differing from the sources reported in the literature, such as demolition and laboratory. A characterization of RCP-C was performed, and the hydration, fresh and hardened state properties of cement pastes with RCP-C were studied. Based on the presented results, it can be concluded that:

RCP-C has a chemical composition similar to Portland cement, with a higher content of CaO, followed by SiO₂ and Al₂O₃. Although it cannot be considered a pozzolanic material, its physical characteristics allow it to be considered as SCM: particle size distribution close to Portland cement and higher SSA.

Replacing Portland cement with RCP-C significantly decreases the fluidity of pastes, as verified by the spread area, τ_0 , and μ . This behavior is attributed to the irregular morphology of RCP-C particles that generate friction and to the higher SSA that increases the water requirement. The loss of fluidity is considerable for high percentages of RCP, this aspect could cause a non-uniformity of the pastes and an increase in porosity, producing the appearance of cracks or changes in the dimension of the specimens, which would affect the results of the resistance to compression and modulus of elasticity.

The use of RCP-C reduces the induction period and accelerates the hydration of cement pastes at early ages (~3h) due to the nucleation effect. Subsequently, due to clinker dilution, heat flow and accumulated heat reduce as the replacement of Portland cement by RCP-C increases.

Compressive strength shows a reduction at early ages, where dilution effect prevails. However, at later ages (28 and 120 days), the reduction is lower, and the values are even similar between the reference and 10% of RCP-C, which can be attributed to the filling effect and possible pozzolanic activity, as well as rehydration of old cement particles. It is suggested to complement these results with the evaluation of the porosity and the pore index in order to explain their influence on the resistance in the mechanical properties.

The elastic modulus also shows the same behavior, affected by dilution and physical characteristics of RCP-C. The use of RCP-C is feasible as a substitute for Portland cement. However, it is necessary to consider the additions that the cement may have in order to consider the synergistic effect of the materials (including RCP-C). To improve the fluidity of cement-based materials, it is recommended to consider superplasticizer additives. Although it reduces compressive strength and modulus of elasticity, using lower percentages of RCP-C (~10%) and higher

fineness ($< D_{50}=14.42 \mu\text{m}$) would improve its mechanical behavior.

AUTHOR CONTRIBUTIONS:

Conceptualization: J.H.A. Rocha, R.D. Toledo Filho. Data cleansing: J.H.A. Rocha. Formal analysis: J.H.A. Rocha, M.P. Tinoco. Funding raising: R.D. Toledo Filho. Research: J.H.A. Rocha. Methodology: J.H.A. Rocha, M.P. Tinoco. Project administration: R.D. Toledo Filho. Resources: R.D. Toledo Filho. Supervision: R.D. Toledo Filho. Validation: J.H.A. Rocha. Visualization: J.H.A. Rocha, M.P. Tinoco. Writing, original draft: J.H.A. Rocha, M.P. Tinoco. Writing, review & editing: J.H.A. Rocha, M.P. Tinoco, R.D. Toledo Filho.

REFERENCES

- Rahla, K.M.; Mateus, R.; Bragança, L. (2019) Comparative sustainability assessment of binary blended concretes using Supplementary Cementitious Materials (SCMs) and Ordinary Portland Cement (OPC). *J. Clean. Prod.* 220, 445–459. <https://doi.org/10.1016/j.jclepro.2019.02.010>.
- Ashish, D.K. (2019) Concrete made with waste marble powder and supplementary cementitious material for sustainable development. *J. Clean. Prod.* 211, 716–729. <https://doi.org/10.1016/j.jclepro.2018.11.245>.
- Lothenbach, B.; Scrivener, K.; Hooton, R.D. (2011) Supplementary cementitious materials. *Cem. Concr. Res.* 41 [12], 1244–1256. <https://doi.org/10.1016/j.cemconres.2010.12.001>.
- Juenger, M.C.G.; Snellings, R.; Bernal, S.A. (2019) Supplementary cementitious materials: New sources, characterization, and performance insights. *Cem. Concr. Res.* 122, 257–273. <https://doi.org/10.1016/j.cemconres.2019.05.008>.
- de Matos, P.R.; Sakata, R.D.; Onghero, L.; Uliano, V.G.; de Brito, J.; Campos, C.E.M.; Gleize, P.J.P. (2021) Utilization of ceramic tile demolition waste as supplementary cementitious material: An early-age investigation. *J. Build. Eng.* 38, 102187. <https://doi.org/10.1016/j.jobte.2021.102187>.
- Suraneni, P.; Hajibabae, A.; Ramanathan, S.; Wang, Y.; Weiss, J. (2019) New insights from reactivity testing of supplementary cementitious materials. *Cem. Concr. Compos.* 103, 331–338. <https://doi.org/10.1016/j.cemconcomp.2019.05.017>.
- Menegaki, M.; Damigos, D. (2018) A review on current situation and challenges of construction and demolition waste management. *Curr. Opin. Green Sustain. Chem.* 13, 8–15. <https://doi.org/10.1016/j.cogsc.2018.02.010>.
- Li, Y.; Zhang, X.; Ding, G.; Feng, Z. (2016) Developing a quantitative construction waste estimation model for building construction projects. *Resour. Conserv. Recycl.* 106, 9–20. <https://doi.org/10.1016/j.resconrec.2015.11.001>.
- Wu, H.; Yang, D.; Xu, J.; Liang, C.; Ma, Z. (2021) Water transport and resistance improvement for the cementitious composites with eco-friendly powder from various concrete wastes. *Constr. Build. Mater.* 290, 123247. <https://doi.org/10.1016/j.conbuildmat.2021.123247>.
- Wang, H.; Wang, L.; Shen, W.; Cao, K.; Sun, L.; Wang, P.; Cui, L. (2022) Compressive strength, hydration and pore structure of alkali-activated slag mortars integrating with recycled concrete powder as binders. *KSCE J. Civ. Eng.* 26, 795–805. <https://doi.org/10.1007/s12205-021-0406-1>.
- Liu, C.; Liu, H.; Wu, J. (2022) Effect of recycled mixed powder on the mechanical properties and microstructure of concrete. *J. Renew. Mater.* 10 [5], 1397–1414. <https://doi.org/10.32604/jrm.2022.018386>.
- Tang, Q.; Ma, Z.; Wu, H.; Wang, W. (2020) The utilization of eco-friendly recycled powder from concrete and brick waste in new concrete: A critical review. *Cem. Concr. Compos.* 114, 103807. <https://doi.org/10.1016/j.cemconcomp.2020.103807>.

13. Likes, L.; Markandeya, A.; Haider, M.M.; Bollinger, D.; McCloy, J.S.; Nassiri, S. (2022) Recycled concrete and brick powders as supplements to Portland cement for more sustainable concrete. *J. Clean. Prod.* 364, 132651. <https://doi.org/10.1016/j.jclepro.2022.132651>.
14. Rangel, C.S.; Toledo Filho, R.D.; Amario, M.; Pepe, M.; de Castro Polisseni, G.; Puente de Andrade, G. (2019) Generalized quality control parameter for heterogenous recycled concrete aggregates: A pilot scale case study. *J. Clean. Prod.* 208, 589–601. <https://doi.org/10.1016/j.jclepro.2018.10.110>.
15. Oliveira, T.C.F.; Dezen, B.G.S.; Possan, E. (2020) Use of concrete fine fraction waste as a replacement of Portland cement. *J. Clean. Prod.* 273, 123126. <https://doi.org/10.1016/j.jclepro.2020.123126>.
16. Oh, D.; Noguchi, T.; Kitagaki, R.; Choi, H. (2021) Proposal of demolished concrete recycling system based on performance evaluation of inorganic building materials manufactured from waste concrete powder. *Renew. Sust. Energ. Rev.* 135, 110147. <https://doi.org/10.1016/j.rser.2020.110147>.
17. Oksri-Nelfia, L.; Mahieux, P.Y.; Amiri, O.; Turcry, P.; Lux, J. (2016) Reuse of recycled crushed concrete fines as mineral addition in cementitious materials. *Mater. Struct.* 49, 3239–3251. <https://doi.org/10.1617/s11527-015-0716-1>.
18. Cantero, B.; Bravo, M.; de Brito, J.; Del Bosque, I.F.S.; Medina, C. (2022) The influence of fly ash on the mechanical performance of cementitious materials produced with recycled cement. *Appl. Sci.* 12 [4], 12042257. <https://doi.org/10.3390/app12042257>.
19. Deng, X.; Guo, H.; Tan, H.; He, X.; Zheng, Z.; Su, Y.; Yang, J. (2021) An accelerator prepared from waste concrete recycled powder and its effect on hydration of cement-based materials. *Constr. Build. Mater.* 296, 123767. <https://doi.org/10.1016/j.conbuildmat.2021.123767>.
20. Chen, X.; Li, Y.; Bai, H.; Ma, L. (2021) Utilization of recycled concrete powder in cement composite: Strength, microstructure and hydration characteristics. *J. Renew. Mater.* 9 [12], 2189–2208. <https://doi.org/10.32604/jrm.2021.015394>.
21. Hou, S.; Xiao, J.; Duan, Z.; Ma, G. (2021) Fresh properties of 3D printed mortar with recycled powder. *Constr. Build. Mater.* 309, 125186. <https://doi.org/10.1016/j.conbuildmat.2021.125186>.
22. Kim, J.; Jang, H. (2022) Closed-loop recycling of C&D waste: Mechanical properties of concrete with the repeatedly recycled C&D powder as partial cement replacement. *J. Clean. Prod.* 343, 130977. <https://doi.org/10.1016/j.jclepro.2022.130977>.
23. Ma, Z.; Yao, P.; Yang, D.; Shen, J. (2021) Effects of fire-damaged concrete waste on the properties of its preparing recycled aggregate, recycled powder and newmade concrete. *J. Mater. Res. Technol.* 15, 1030–1045. <https://doi.org/10.1016/j.jmrt.2021.08.116>.
24. Xiao, J.; Ma, Z.; Sui, T.; Akbarnezhad, A.; Duan, Z. (2018) Mechanical properties of concrete mixed with recycled powder produced from construction and demolition waste. *J. Clean. Prod.* 188, 720–731. <https://doi.org/10.1016/j.jclepro.2018.03.277>.
25. Mehdizadeh, H.; Cheng, X.; Mo, K.H.; Ling, T.C. (2022) Upcycling of waste hydrated cement paste containing high-volume supplementary cementitious materials via CO₂ pre-treatment. *J. Build. Eng.* 52, 104396. <https://doi.org/10.1016/j.jobe.2022.104396>.
26. Horsakulthai, V. (2021) Effect of recycled concrete powder on strength, electrical resistivity, and water absorption of self-compacting mortars. *Case Stud. Constr.* 15, e00725. <https://doi.org/10.1016/j.cscm.2021.e00725>.
27. Letelier, V.; Tarela, E.; Muñoz, P.; Moriconi, G. (2017) Combined effects of recycled hydrated cement and recycled aggregates on the mechanical properties of concrete. *Constr. Build. Mater.* 132, 365–375. <https://doi.org/10.1016/j.conbuildmat.2016.12.010>.
28. Zhang, J.; Tan, H.; He, X.; Zhao, R.; Yang, J.; Su, Y. (2021) Nano particles prepared from hardened cement paste by wet grinding and its utilization as an accelerator in Portland cement. *J. Clean. Prod.* 283, 124632. <https://doi.org/10.1016/j.jclepro.2020.124632>.
29. Yang, J.; Zeng, L.; Su, Z.; He, X.; Su, Y.; Zhao, R.; Gan, X. (2020) Wet-milling disposal of autoclaved aerated concrete demolition waste – A comparison with classical supplementary cementitious materials. *Adv. Powder Technol.* 31 [9], 3736–3746. <https://doi.org/10.1016/j.apt.2020.07.016>.
30. Prošek, Z.; Trejbal, J.; Nežerka, V.; Goliáš, V.; Faltus, M.; Tesárek, P. (2020) Recovery of residual anhydrous clinker in finely ground recycled concrete. *Resour. Conserv. Recycl.* 155, 104640. <https://doi.org/10.1016/j.resconrec.2019.104640>.
31. He, Z.; Han, X.; Zhang, M.; Yuan, Q.; Shi, J.; Zhan, P. (2022) A novel development of green UHPC containing waste concrete powder derived from construction and demolition waste. *Powder Technol.* 398, 117075. <https://doi.org/10.1016/j.powtec.2021.117075>.
32. He, X.; Zheng, Z.; Yang, J.; Su, Y.; Wang, T.; Strnadl, B. (2020) Feasibility of incorporating autoclaved aerated concrete waste for cement replacement in sustainable building materials. *J. Clean. Prod.* 250, 119455. <https://doi.org/10.1016/j.jclepro.2019.119455>.
33. Sun, C.; Chen, L.; Xiao, J.; Liu, Q.; Zuo, J. (2021) Low-Carbon and fundamental properties of eco-efficient mortar with recycled powders. *Materials* 14 [24], 7503. <https://doi.org/10.3390/ma14247503>.
34. Wu, H.; Xu, J.; Yang, D.; Ma, Z. (2021) Utilizing thermal activation treatment to improve the properties of waste cementitious powder and its newmade cementitious materials. *J. Clean. Prod.* 322, 129074. <https://doi.org/10.1016/j.jclepro.2021.129074>.
35. ABNT (2018). NBR 16697: Cimento portland — requisitos. ABNT, Rio de Janeiro.
36. Kaliyavaradhan, S.K.; Li, L.; Ling, T.-C. (2022) Response surface methodology for the optimization of CO₂ uptake using waste concrete powder. *Constr. Build. Mater.* 340, 127758. <https://doi.org/10.1016/j.conbuildmat.2022.127758>.
37. Li, X.; Lv, X.; Zhou, X.; Meng, W.; Bao, Y. (2022) Upcycling of waste concrete in eco-friendly strain-hardening cementitious composites: Mixture design, structural performance, and life-cycle assessment. *J. Clean. Prod.* 330, 129911. <https://doi.org/10.1016/j.jclepro.2021.129911>.
38. ABNT (2012). NBR NM18: Cimento portland - análise química - determinação de perda ao fogo. abnt, rio de janeiro.
39. ASTM (2019). ASTM C204: Standard test methods for fineness of hydraulic cement by air-permeability apparatus. ASTM: West Conshohocken, PA, USA, 2019.
40. ABNT (2019). NBR7215: Cimento portland - determinação da resistência à compressão de corpos de prova cilíndricos. ABNT, Rio de Janeiro.
41. Tinoco, M.P.; Gouvêa, L.; de Cássia Magalhães Martins, K.; Dias Toledo Filho, R.; Aurelio Mendoza Reales, O. (2023) The use of rice husk particles to adjust the rheological properties of 3D printable cementitious composites through water sorption. *Constr. Build. Mater.* 365, 130046. <https://doi.org/10.1016/j.conbuildmat.2022.130046>.
42. ASTM (2022). ASTM C469/C469M-22: Standard test method for static modulus of elasticity and poisson's ratio of concrete in compression. ASTM, West Conshohocken.
43. Prošek, Z.; Nežerka, V.; Hlůžek, R.; Trejbal, J.; Tesárek, P.; Karra'a, G. (2019) Role of lime, fly ash, and slag in cement pastes containing recycled concrete fines. *Constr. Build. Mater.* 201, 702–714. <https://doi.org/10.1016/j.conbuildmat.2018.12.227>.
44. ASTM (2022). ASTM C618-22: Standard specification for coal fly ash and raw or calcined natural pozzolan for use in concrete. ASTM, West Conshohocken.
45. Gao, Y.; Cui, X.; Lu, N.; Hou, S.; He, Z.; Liang, C. (2022) Effect of recycled powders on the mechanical properties and durability of fully recycled fiber-reinforced mortar. *J. Build. Eng.* 45, 103574. <https://doi.org/10.1016/j.jobe.2021.103574>.
46. Real, S.; Bogas, J.A.; Carriço, A.; Hu, S. (2021) Mechanical characterisation and shrinkage of thermoactivated recycled cement concrete. *Appl. Sci.* 11 [6], 11062454. <https://doi.org/10.3390/app11062454>.
47. Shen, P.; Sun, Y.; Liu, S.; Jiang, Y.; Zheng, H.; Xuan, D.; Lu, J.; Poon, C.S. (2021) Synthesis of amorphous nano-silica from recycled concrete fines by two-step wet carbonation. *Cem. Concr. Res.* 147, 106526. <https://doi.org/10.1016/j.cemconres.2021.106526>.

48. Liu, M.; Wu, H.; Yao, P.; Wang, C.; Ma, Z. (2022) Microstructure and macro properties of sustainable alkali-activated fly ash mortar with various construction waste fines as binder replacement up to 100%. *Cem. Concr. Compos.* 134, 104733. <https://doi.org/10.1016/j.cemconcomp.2022.104733>
49. Qin, L.; Gao, X. (2019) Recycling of waste autoclaved aerated concrete powder in Portland cement by accelerated carbonation. *Waste Manage.* 89, 254–264. <https://doi.org/10.1016/j.wasman.2019.04.018>.
50. Sui, Y.; Ou, C.; Liu, S.; Zhang, J.; Tian, Q. (2020) Study on properties of waste concrete powder by thermal treatment and application in mortar. *Appl. Sci.* 10 [3], 10030998. <https://doi.org/10.3390/app10030998>.
51. Chen, X.; Li, Y.; Zhu, Z.; Ma, L. (2022) Evaluation of waste concrete recycled powder (WCRP) on the preparation of low-exothermic cement. *J. Build. Eng.* 53, 104511. <https://doi.org/10.1016/j.jobe.2022.104511>.
52. Li, S.; Gao, J.; Li, Q.; Zhao, X. (2021) Investigation of using recycled powder from the preparation of recycled aggregate as a supplementary cementitious material. *Constr. Build. Mater.* 267, 120976. <https://doi.org/10.1016/j.conbuildmat.2020.120976>.
53. Ma, Z.; Shen, J.; Wu, H.; Zhang, P. (2022) Properties and activation modification of eco-friendly cementitious materials incorporating high-volume hydrated cement powder from construction waste. *Constr. Build. Mater.* 316, 125788. <https://doi.org/10.1016/j.conbuildmat.2021.125788>.
54. Ge, Z.; Gao, Z.; Sun, R.; Zheng, L. (2012) Mix design of concrete with recycled clay-brick-powder using the orthogonal design method. *Constr. Build. Mater.* 31, 289–293. <https://doi.org/10.1016/j.conbuildmat.2012.01.002>.
55. Moreno-Juez, J.; Vegas, I.J.; Frías Rojas, M.; Vigil de la Villa, R.; Guede-Vázquez, E. (2021) Laboratory-scale study and semi-industrial validation of viability of inorganic CDW fine fractions as SCMs in blended cements. *Constr. Build. Mater.* 271, 121823. <https://doi.org/10.1016/j.conbuildmat.2020.121823>.
56. Wang, T.; He, X.; Yang, J.; Zhao, H.; Su, Y. (2020) Nano-treatment of autoclaved aerated concrete waste and its usage in cleaner building materials. *Journal of Wuhan University of Technology-Mater. Sci. Ed.* 35, 786-793. <https://doi.org/10.1007/s11595-020-2321-6>.
57. Wang, L.; Wang, J.; Wang, H.; Fang, Y.; Shen, W.; Chen, P.; Xu, Y. (2022) Eco-friendly treatment of recycled concrete fines as supplementary cementitious materials. *Constr. Build. Mater.* 322, 126491. <https://doi.org/10.1016/j.conbuildmat.2022.126491>.
58. Liu, X.; Liu, L.; Lyu, K.; Li, T.; Zhao, P.; Liu, R.; Zuo, J.; Fu, F.; Shah, S.P. (2022) Enhanced early hydration and mechanical properties of cement-based materials with recycled concrete powder modified by nano-silica. *J. Build. Eng.* 50, 104175. <https://doi.org/10.1016/j.jobe.2022.104175>.
59. Dun, Z.; Wang, M.; Ren, L.; Dun, Z. (2021) Tests research on grouting materials of waste-concrete-powder cement for goaf ground improvement. *Adv. Mater. Sci. Eng.* 2021, 9598418. <https://doi.org/10.1155/2021/9598418>.
60. Singh, A.; Arora, S.; Sharma, V.; Bhardwaj, B. (2019) Workability retention and strength development of self-compacting recycled aggregate concrete using ultrafine recycled powders and silica fume. *J. Hazard. Toxic Radioact. Waste* 23 [4], 04019016. [https://doi.org/10.1061/\(asce\)hz.2153-5515.0000456](https://doi.org/10.1061/(asce)hz.2153-5515.0000456).
61. Liang, G.; Liu, T.; Li, H.; Wu, K. (2022) Shrinkage mitigation, strength enhancement and microstructure improvement of alkali-activated slag/fly ash binders by ultrafine waste concrete powder. *Compos. B Eng.* 231, 109570. <https://doi.org/10.1016/j.compositesb.2021.109570>.
62. Tang, Y.; Xiao, J.; Zhang, H.; Duan, Z.; Xia, B. (2022) Mechanical properties and uniaxial compressive stress-strain behavior of fully recycled aggregate concrete. *Constr. Build. Mater.* 323, 126546. <https://doi.org/10.1016/j.conbuildmat.2022.126546>.
63. Wang, D.; Shi, C.; Farzadnia, N.; Shi, Z.; Jia, H.; Ou, Z. (2018) A review on use of limestone powder in cement-based materials: Mechanism, hydration and microstructures. *Constr. Build. Mater.* 181, 659-672. <https://doi.org/10.1016/j.conbuildmat.2018.06.075>.
64. Benachour, Y.; Davy, C.A.; Skoczylas, F.; Houari, H. (2008) Effect of a high calcite filler addition upon microstructural, mechanical, shrinkage and transport properties of a mortar. *Cem. Concr. Res.* 38 [6], 727-736. <https://doi.org/10.1016/j.cemconres.2008.02.007>.
65. Bogas, J.A.; Carriço, A.; Pereira, M.F.C. (2019) Mechanical characterization of thermal activated low-carbon recycled cement mortars. *J. Clean. Prod.* 218, 377–389. <https://doi.org/10.1016/j.jclepro.2019.01.325>.
66. Zhang, H.; Xiao, J.; Tang, Y.; Duan, Z.; Poon, C. (2022) Long-term shrinkage and mechanical properties of fully recycled aggregate concrete: Testing and modelling. *Cem. Concr. Compos.* 130, 104527. <https://doi.org/10.1016/j.cemconcomp.2022.104527>.
67. Wu, Y.; Mehdizadeh, H.; Mo, K.H.; Ling, T.C. (2022). High-temperature CO₂ for accelerating the carbonation of recycled concrete fines. *J. Build. Eng.* 52, 104526. <https://doi.org/10.1016/j.jobe.2022.104526>.
68. Caneda-Martínez, L.; Monasterio, M.; Moreno-Juez, J.; Martínez-Ramírez, S.; García, R.; Frías, M. (2021) Behaviour and properties of eco-cement pastes elaborated with recycled concrete powder from construction and demolition wastes. *Materials* 14 [5], 1299. <https://doi.org/10.3390/ma14051299>.
69. Real, S.; Carriço, A.; Bogas, J.A.; Guedes, M. (2020) Influence of the treatment temperature on the microstructure and hydration behavior of thermoactivated recycled cement. *Materials*. 13 [18], 3937. <https://doi.org/10.3390/ma13183937>.